SURFACE AND ANTICORROSION PROPERTIES OF HYDROPHOBIC AND HYDROPHILIC TiO$_2$ COATINGS ON A STAINLESS-STEEL SUBSTRATE

POVRŠINSKE IN PROTIKOROZIJSKE LASTNOSTI HIDROFOBNIH IN HIDROFILNIH TiO$_2$ PREVLEK NA JEKLENI PODLAGI

Marjetka Conradi, Aleksandra Kocijan

Institute of Metals and Technology, Lepi pot 11, 1000 Ljubljana, Slovenia
marjetka.conradi@imt.si

We compare the wetting, morphology and anticorrosion properties of fluorosilane-modified TiO$_2$ (FAS-TiO$_2$/epoxy) and as-received TiO$_2$/epoxy coatings. An array of double-layer TiO$_2$ nanoparticles of two sizes (30 nm and 300 nm) were spin coated onto a steel substrate AISI 316L. The static water contact angles were measured to evaluate the wetting properties of the FAS-TiO$_2$/epoxy (hydrophobic) and the as-received TiO$_2$/epoxy (hydrophilic) coatings. The morphology of the coatings was analyzed with average surface roughness (S_a) measurements and SEM imaging. We show that the order of the deposition in a double layer composed of dual-size nanoparticles plays an important role in the surface roughness and hence the wettability. SEM images reveal a typical morphology and S_a difference between the FAS-TiO$_2$/epoxy and the as-received TiO$_2$/epoxy coatings, reflected in the discrepancy of the average size of the agglomerates that are coating the substrate. Potentiodynamic measurements show an enhanced corrosion resistance for the FAS-TiO$_2$/epoxy-coated AISI 316L stainless steel compared to the as-received TiO$_2$/epoxy-coated AISI 316L.

Keywords: TiO$_2$, epoxy, coatings, wetting, corrosion

V članku primerjamo omočitvene lastnosti, morfologijo in antikorozijske lastnosti s fluorosilanom oblečenih TiO$_2$ (FAS-TiO$_2$/epoksi) in čistih TiO$_2$/epoksi prevlek. TiO$_2$ nanodelce dveh velikosti (30 nm in 300 nm) smo na jekleno podlago tipa AISI 316L nanesli s "spin coaterjem". Omočitvene lastnosti prevlek smo določili z meritvami statičnih kontaktnih kotov. Le-te so pokazale hidrofobno naravo FAS-TiO$_2$/epoksi prevlek in hidorfilno naravo čistih TiO$_2$/epoksi prevlek. Morfološke lastnosti prevlek smo analizirali z meritvami povprečne hrapavosti površine (S_a) ter SEM-mikroskopijo. Pokazali smo pomen vrstnega reda nalaganja nanodelcev dveh velikosti na hrapavost površin in njeno omočljivost. SEM-posnetki prikazujejo razliko v morfologiji in hrapavosti površin FAS-TiO$_2$/epoksi in čistih TiO$_2$/epoksi prevlek, ki se odraža v tvorbi aglomeratov različnih velikosti na eni in drugi površini. Potenciodinamske meritve kažejo izboljšano odpornost proti koroziji FAS-TiO$_2$/epoksi prevlek v primerjavi s čistimi TiO$_2$/epoksi prevlekami na jekleni podlagi tipa AISI 316L.

Ključne besede: TiO$_2$, epoksi, prevleke, omočitvene lastnosti, korozija

1 INTRODUCTION

Austenitic (AISI) stainless steel is an important engineering material because of its generally high corrosion resistance combined with favourable mechanical properties, such as its high tensile strength.[1,2] Its high corrosion resistance is attributed to the presence of a passive film, which is stable, invisible, thin, durable and extremely adherent and self-repairing.[3] However, in many aggressive environments, such as a chloride-ion-rich environment, AISI 316L stainless steel is still observed to suffer from pitting corrosion.[4] Therefore, the modification of metallic surfaces using various coatings is an important subject in the field of enhancing particular surface properties, mechanical as well as anticorrosion properties.

Epoxy coatings have been widely used for metallic-surface protection because of their good mechanical and electrical-insulating properties, chemical resistance and strong adhesion to heterogeneous substrates. However, the highly cross-linked structure of an epoxy resin often makes epoxy coatings susceptible to the propagation of cracks and damage due to surface abrasion and wear.[5] Therefore, a lot of research has been done to improve the performance of epoxy coatings by adding various nanoparticles, like SiO$_2$, TiO$_2$, ZnO, CuO etc.[6] In addition, nanoparticles also enhance the corrosion-protection properties of the epoxy coatings by decreasing the porosities due to the small size and high specific area. TiO$_2$ nanoparticles are well-known anticorrosion additives used in several applications, such as aerospace, marine, biomedicine, etc. because of their unique physiochemical properties and good chemical stability.[7–9]

Here we report on a comparison of the surface and anticorrosion properties of double-layer, dual-size (30 nm and 300 nm) FAS-TiO$_2$/epoxy and as-received TiO$_2$/epoxy coatings. We show that the order of the nanoparticle deposition plays an important role in the wetting and the morphological properties of the coatings. Potentiodynamic measurements reveal that the hydrophobic coating has better anticorrosion properties than the hydrophilic coating.

2 EXPERIMENTAL PART

Materials – Epoxy resin (Epikote 816, Momentive Specialty Chemicals B.V.) was mixed with a hardener Epikure F205 (Momentive Specialty Chemicals B.V.) in the ratio of mass fractions of 100:53 %. TiO_2 nanoparticles with mean diameters of 30 nm were provided by Cinkarna Celje, whereas the 300-nm particles were provided by US Research Nanomaterials, Inc.

Austenitic stainless steel AISI 316L (17 % Cr, 10 % Ni, 2.1 % Mo, 1.4 % Mn, 0.38 % Si, 0.041 % P, 0.021 % C, <0.005 % S in mass fraction) was used as a substrate.

Surface functionalization – For the hydrophobic effect, TiO_2 particles were functionalized in 1 % of volume fractions of ethanolic fluoroalkylsilane or FAS17 ($C_{16}H_{19}F_{17}O_3Si$) solution.

Steel substrate preparation – Prior to the application of the coating, the steel discs of 25 mm diameter and with a thickness of 1.5 mm were diamond polished following a standard mechanical procedure and then cleaned with ethanol in an ultrasonic bath.

Coating preparation – To improve the TiO_2 nanoparticles' adhesion, the diamond-polished AISI 316L substrate was spin-coated with a 300-nm layer of epoxy (as determined by ellipsometry)[10] and then cured for 1 h at 70 °C and post-cured at 150 °C for another hour. The nanoparticles were then coated onto the AISI 316L + epoxy (AISI + E) surface by spin-coating 20 μL of 3 % of mass fractions of TiO_2 nanoparticle ethanolic solution. We prepared dual-size, double-layer coatings consisting of 30 nm and 300 nm FAS-TiO_2 nanoparticles. Both possibilities of the order of TiO_2 nanoparticles were analyzed for the FAS-TiO_2/epoxy coatings' preparation: AISI+E+30+300 and AISI+E+300+30. Finally, the coatings were dried in an oven for approximately 20 min at 100 °C.

The same procedure was repeated with the as-received, non-functionalized, TiO_2 nanoparticles to prepare the TiO_2/epoxy coatings.

Scanning electron microscopy (*SEM*) – SEM analysis using a FE-SEM Zeiss SUPRA 35VP was employed to investigate the morphology of the TiO_2 coatings' surfaces, which were sputtered with gold prior to imaging.

Contact-angle measurements – The static contact-angle measurements of water (W) on the TiO_2/epoxy-coated AISI 316L substrates and on the FAS-TiO_2/epoxy-coated AISI 316L substrates were performed using a surface-energy evaluation system (Advex Instruments s.r.o.). Liquid drops of 5 μL were deposited on different spots of the substrates to avoid the influence of roughness and gravity on the shape of the drop. The drop contour was analysed from an image of the deposited liquid drop on the surface and the contact angle was determined by using Young-Laplace fitting. To minimize the errors due to roughness and heterogeneity, the average values of the contact angles of the drop were calculated approximately 30 s after the deposition from at least five measurements on the studied coated steel. All the contact-angle measurements were carried out at 20 °C and ambient humidity.

Surface roughness – Optical 3D metrology system, model Alicona Infinite Focus (Alicona Imaging GmbH) was employed for the surface-roughness analysis. At least three measurements per sample were performed at a magnification of 20× with a lateral resolution of 0.9 μm and a vertical resolution of about 50 nm. IF-Measure-Suite (Version 5.1) software was used for the roughness analysis. The software offers the possibility to calculate the average surface roughness, S_a, for each sample, based on the general surface roughness equation (Equation 1):

$$Sa = \frac{1}{L_x} \frac{1}{L_y} \int_0^{L_x} \int_0^{L_y} |z(x,y)| \mathrm{d}x \mathrm{d}y \qquad (1)$$

where L_x and L_y are the acquisition lengths of the surface in the *x* and *y* directions and $z(x,y)$ is the height. The size of the analyzed area was (714×542) μm. To level the profile, corrections were made to exclude the general geometrical shape and possible measurement-induced misfits.

Electrochemical measurements – Electrochemical measurements were performed on the TiO_2/epoxy-coated AISI 316L stainless steel and on the FAS-TiO_2/epoxy-coated AISI 316L stainless steel. The experiments were carried out in a simulated physiological Hank's solution, containing 8 g/L NaCl, 0.40 g/L KCl, 0.35 g/L $NaHCO_3$, 0.25 g/L $NaH_2PO_4×2H_2O$, 0.06 g/L $Na_2HPO_4×2H_2O$, 0.19 g/L $CaCl_2×2H_2O$, 0.41 g/L $MgCl_2×6H_2O$, 0.06 g/L $MgSO_4×7H_2O$ and 1 g/L glucose, at pH = 7.8 and 37 °C. All the chemicals were from Merck, Darmstadt, Germany. The measurements were performed by using BioLogic Modular Research Grade Potentiostat/Galvanostat/FRA Model SP-300 with EC-Lab Software and a three-electrode flat corrosion cell, where the working electrode (WE) was the investigated specimen, the reference electrode (RE) was a saturated calomel electrode (SCE, 0.242 V vs. SHE) and the counter electrode (CE) was a platinum net. The specimens were immersed in the solution 1 h prior to the measurement in order to stabilize the surface at the open-circuit potential (OCP). The potentiodynamic curves were recorded, starting the measurement at 250 mV vs. SCE more negative than the open-circuit potential (OCP). The potential was then increased, using a scan rate of 1 mV s^{-1}, until the transpassive region was reached.

3 RESULTS AND DISCUSSION

3.1 Wetting properties

To analyze the surface wettability, we performed five static contact-angle measurements with water (W) on different spots all over the sample and used them to determine the average contact-angle values of the coating with an estimated error in the reading of $\theta \pm 1.0°$.

To fabricate a surface that is as hydrophobic as possible we followed the trend of increasing hydrophobicity based on dual-scale roughness.[11,12] For this purpose, the surface roughness was adjusted via spin-coating 30-nm

and 300-nm FAS-TiO$_2$ nanoparticles onto the flat AISI+E surface. The substrate was consequently modified by self-assembled FAS-TiO$_2$ nanoparticles resulting in micro- to nanoparticle-textured surfaces with a refined roughness structure. The static water contact angles, θ^W, and average surface roughness, S_a, for both possibilities of the dual-size, double-layer, FAS-TiO$_2$/epoxy coatings, (30 + 300) nm and reversed, (300 + 30) nm, are listed in **Table 1**. The measured contact angles indicate that the surface is more hydrophobic when the bottom layer is composed of 30-nm and the top layer of 300-nm FAS-TiO$_2$. The difference in θ^W between the two coatings is approximately 11° and this behavior can be attributed to the increased roughness implemented by the larger nanoparticles on the top, which is reflected in the average surface-roughness measurements, S_a (**Table 1**).

Table 1: Comparison of static water contact angles (θ^W) and average surface roughness (S_a) of dual-size, double-layer FAS-TiO$_2$/epoxy and as-received TiO$_2$/epoxy coatings
Tabela 1: Primerjava statičnih kontaktnih kotov (θ^W) in povprečne površinske hrapavosti (S_a) dvoplastnih FAS-TiO$_2$/epoksi in čistih TiO$_2$/epoksi prevlek

	Contact angle	Rough-ness	Contact angle	Rough-ness
	FAS-TiO$_2$		TiO$_2$	
Substrate	θ^W/°	S_a/nm	θ^W/°	S_a/nm
AISI+E+30+300	126.0	250.9	80.3	89.8
AISI+E+300+30	115.2	160.2	79.2	95.1

We prepared, in the same manner, a double-layer of (30 + 300) nm and (300 + 30) nm with as-received TiO$_2$, nanoparticles. These coatings are hydrophilic due to the hydroxyl groups on the surface of the as-received TiO$_2$ nanoparticles. The static water contact angles of both possibilities were comparable, around 80°. In addition, the average surface roughness, S_a, was much lower compared to the FAS-TiO$_2$/epoxy coatings (**Table 1**). This result indicates that FAS functionalization significantly changes not only the wetting properties of the coating but also its morphology, as will be shown in the following section.

3.2 Surface morphology

Figure 1 compares the morphology of the double-layer FAS-TiO$_2$/epoxy (a, b) and the as-received TiO$_2$/epoxy (c, d) coatings. SEM images reveal an obvious difference in the morphology between layers of FAS-TiO$_2$ and as-received TiO$_2$ nanoparticles, which is reflected mostly in the different length scale of the average size of the nanoparticle agglomerates and consequently in a discrepancy of the average surface roughness, S_a, as reported in **Table 1**. FAS functionalization apparently does not homogenize the particle distribution as the formation of large agglomerates up to a few tenths of microns is observed (**Figure 1a** and **1b**). In contrast, for the as-received TiO$_2$ nanoparticle coatings, the nanoparticles are more finely dispersed and agglomerates of

the order of few microns are observed (**Figure 1c** and **1d**).

SEM images also reveal that TiO$_2$ nanoparticles were not able to cover completely the underlying substrate This might additionally influence the contact-angle values and the wetting properties of the FAS-TiO$_2$ and the as-received TiO$_2$ layers as the epoxy substrate is hydrophilic with a static water contact angle of 74.3°. This effect is, however, probably more pronounced in coatings prepared with hydrophobic FAS-TiO$_2$ nanoparticles, as the uncovered fractions allow the water to impregnate between the nanoparticles and the agglomerates to come into contact with the exposed hydrophilic epoxy and, consequently, reduce the static water contact angle. On the other hand, this effect does not play an important role in the as-received TiO$_2$/epoxy coatings as both the as-received TiO$_2$ nanoparticles and the epoxy are hydrophilic.

The role of the order of nanoparticle deposition seems to be more pronounced in the FAS-TiO$_2$/epoxy coatings (**Figure 1a** and **1b**), which is also reflected in the discrepancy in static water contact angles and the average surface roughness between AISI+E+30+300 and AISI+E+300+30, as reported in **Table 1**. Larger particles on the top seem to create larger agglomerates and consequently a rougher surface.

The morphology of the as-received TiO$_2$/epoxy coatings, AISI+E+30+300 and AISI+E+300+30 (**Figure 1c** and **1d**) is, however, comparable, as are the static water contact angles and the average surface roughness (**Table 1**).

3.3 Potentiodynamic measurements

For an analysis of the anticorrosion properties we chose the more hydrophobic coating, FAS-TiO$_2$/epoxy coating, AISI+E+30+300. The comparison was made
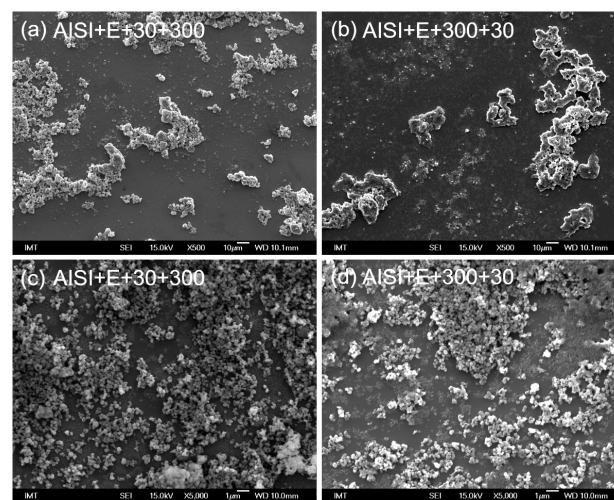
Figure 1: Comparison of surface morphology of double-layer, FAS-TiO$_2$/epoxy (a, b) and as-received, TiO$_2$/epoxy (c, d) coatings
Slika 1: Primerjava morfologije dvoplastnih FAS-TiO$_2$/epoksi (a, b) in čistih TiO$_2$/epoksi (c, d) prevlek
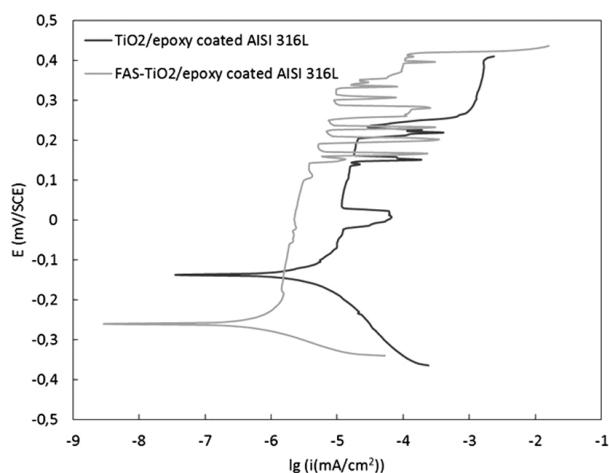
Figure 2: Potentiodynamic curves for as-received TiO_2/epoxy- and FAS-TiO_2/epoxy-coated AISI 316L substrate in a simulated physiological Hank's solution

Slika 2: Potenciodinamske krivulje čistih TiO_2/epoksi in FAS-TiO_2/epoksi prevlek na AISI 316L podlagi, izmerjene v simulitani fiziološki Hankovi raztopini

with the as-received TiO_2/epoxy coating using the same order of particle deposition (30+300). **Figure 2** shows the potentiodynamic behaviour of the as-received TiO_2/epoxy-coated AISI 316L and FAS-TiO_2/epoxy-coated AISI 316L stainless steel in a simulated physiological Hank's solution. We studied the polarization and the passivation behaviour of the tested material after the surface modification. After 1 h of stabilization at the OCP, the corrosion potential (E_{corr}) for the as-received TiO_2/epoxy-coated AISI 316L in Hank's solution was approximately –0.13 V vs. SCE. Following the Tafel region, the alloy exhibited a broad range of passivity. The breakdown potential (E_b) was approximately 0.25 V vs. SCE. In the case of the FAS-TiO_2/epoxy-coated AISI 316L stainless steel, the E_{corr} in Hank's solution was approximately –0.27 V vs. SCE. The passivation range was significantly broader, i.e., 0.4 V vs. SCE, and at lower corrosion-current densities compared to TiO_2/epoxy-coated AISI 316L specimen. The results show an enhanced corrosion resistance for the FAS-TiO_2/epoxy-coated AISI 316L stainless steel compared to as-received TiO_2/epoxy coated AISI 316L.

4 CONCLUSIONS

We analyzed the wettability behavior of double-sized, double-layer, FAS-functionalized TiO_2 and as-received TiO_2 nanostructured surfaces. We showed that the order of the TiO_2 nanoparticle deposition determines the surface roughness and hence the wettability, as confirmed by the average surface-roughness measurements and the SEM imaging. This effect was more pronounced in coatings with FAS-TiO_2 nanoparticles. The morphology analysis also revealed a typical morphology and S_a difference between the FAS-TiO_2/epoxy and the as-received TiO_2/epoxy coatings reflected in a discrepancy in the

average size of the agglomerates that are coating the substrate. The corrosion stability of double-sized, double-layer, FAS-functionalized TiO_2 and the as-received TiO_2 nanostructured coatings on the surface of the AISI 316L stainless steel was studied in a simulated physiological Hank's solution. The results showed the superior corrosion stability of the FAS-TiO_2/epoxy-coated AISI 316L stainless steel compared to the as-received TiO_2/epoxy-coated AISI 316L.

Acknowledgement

5 REFERENCES

[1] M. A. M. Ibrahim, S. S. A. El Rehim, M. M. Hamza, Corrosion behavior of some austenitic stainless steels in chloride environments, Mat. Chem. Phys., 115 (**2009**), 80–85, doi:10.1016/j.matchemphys.2008.11.016

[2] T. Hryniewicz, R. Rokicki, K. Rokosz, Corrosion characteristics of medical-grade AISI Type 316L stainless steel surface after electropolishing in a magnetic field, Corrosion, 64 (**2008**), 660–665, doi: http://dx.doi.org/10.5006/1.3279927

[3] C. Perez, A. Collazo, M. Izquierdo, P. Merino, X. R. Novoa, Characterisation of the barrier properties of different paint systems, Part II. Non-ideal diffusion and water uptake kinetics, Prog. Org. Coat., 37 (**1999**), 169–177, doi:10.1016/s0300-9440(99)00073-9

[4] C. G. Oliveira, M. G. S. Ferreira, Ranking high-quality paint systems using EIS, Part 1: intact coatings, Corrosion Science, 45 (**2003**), 123–138, doi:10.1016/s0010-938x(02)00088-4

[5] B. Wetzel, F. Haupert, M. Q. Zhang, Epoxy nanocomposites with high mechanical and tribological performance, Comp. Sci. Techn., 63 (**2003**), 2055–2067, doi:10.1016/s0266-3538(03)00115-5

[6] Y. Qing, C. Yang, Y. Sun, Y. Zheng, X. Wang, Y. Shang, L. Wang, C. Liu, Facile fabrication of superhydrophobic surfaces with corrosion resistance by nanocomposite coating of TiO2 and polydimethylsiloxane, Colloids and Surfaces a-Physicochemical and Engineering Aspects, 484 (**2015**), 471–477, doi:10.1016/j.colsurfa.2015.08.024

[7] V. N. Moiseev, Titanium in Russia, Metal Science and Heat Treatment, 47 (**2005**), 371–376, doi:10.1007/s11041-005-0080-9

[8] I. Gurrappa, Characterization of titanium alloy Ti-6Al-4V for chemical, marine and industrial applications. Mat. Charact., 51 (**2003**), 131–139, doi:10.1016/j.matchar.2003.10.006

[9] F. Samanipour, F. M. R. Bayati, F. Golestani-Fard, H. R. Zargar, A. R. Mirhabibi, V. Shoaei-Rad, S. Abbasi, Innovative fabrication of ZrO2-HAp-TiO2 nano/micro-structured composites through MAO/EPD combined method. Materials Letters, 65 (**2011**), 926–928, doi:10.1016/j.matlet.2010.11.039

[10] M. Conradi, G. Intihar, M. Zorko, Mechanical and wetting properties of nanosilica/epoxy-coated stainless steel, Mater. Tehnol., 49 (**2015**), 613–618, doi:10.17222/mit.2015.060

[11] L. Xu, R. G. Karunakaran, J. Guo, S. Yang, Transparent, Superhydrophobic Surfaces from One-Step Spin Coating of Hydrophobic Nanoparticles, Acs Appl. Mat. & Interfaces, 4 (**2012**), 1118–1125, doi:10.1021/am201750h

[12] T. J. Athauda, W. Williams, K. P. Roberts, R. R. Ozer, On the surface roughness and hydrophobicity of dual-size double-layer silica nanoparticles. J. Mat. Sci., 48 (**2013**), 6115–6120, doi:10.1007/s10853-013-7407-5